Anesthesiology 2006; 105:1220–7

Influence of Endothelial Glycocalyx Degradation and Surfactants on Air Embolism Adhesion

David M. Eckmann, Ph.D., M.D., Stephen C. Armstead, B.S.†*

Background: **Microbubble adherence to endothelial cells is enhanced after damage to the glycocalyx. The authors tested the hypothesis that exogenous surfactants delivered intravascularly have differential effects on the rate of restoration of blood flow after heparinase-induced degradation of the endothelial glycocalyx.**

Methods: **Air microbubbles were injected into the rat cremaster microcirculation after perfusion with heparinase or saline and intravascular administration of either saline or one of two surfactants. The surfactants were Pluronic F-127 (Molecular Probes, Eugene, OR) and Perftoran (OJSC SPC Perftoran, Moscow, Russia). Embolism dimensions and dynamics were observed using intravital microscopy.**

Results: **Significant results were that bubbles embolized the largest diameter vessels after glycocalyx degradation. Bubbles embolized smaller vessels in the surfactant treatment groups. The incidence of bubble dislodgement and the magnitude of distal displacement were smallest after glycocalyx degradation alone and largest after surfactant alone. The time to bubble clearance and restoration of blood flow was longest with heparinase alone and shortest with Pluronic F-127 alone.**

Conclusions: **Degradation of the glycocalyx causes air bubbles to adhere to the endothelium more proximally in the arteriolar microcirculation. Surfactants added after glycocalyx degradation and before gas embolization promotes bubble lodging in the distal microcirculation. Surfactants may have a clinical role in reducing embolism bubble adhesion to endothelial cells undergoing glycocalyx disruption.**

THE glycocalyx, or endothelial surface layer, incorporates a wide variety of membrane-bound macromolecules that can interact with blood-borne macromolecules. Blood-borne macromolecules can be free in the plasma, integral to surfaces of leukocytes and platelets, or adsorbed onto the surface of gas embolism bubbles. Surface interactions between the glycocalyx and gas emboli can lead to the formation of adhesion, causing bubbles to lodge in the vasculature.[1] Intravascular bubbles, as can occur with extracorporeal circulation or in decompression sickness, obstruct blood flow, initiate clotting, and activate inflammatory pathways.[2] Short-duration occlusion of cerebral or cardiac vessels as a result may leave a patient with transient or permanent injury.[3–5] Intravascular bubbles can provoke local, regional, and global systemic responses. A compounding factor in critically ill or cardiac surgical patients with compromised circulation is that the glycocalyx is easily disrupted by hypoxia,[6] by use of cold cardioplegia solutions,[7] and with ischemia–reperfusion.[8] Endothelial glycocalyx damage has been shown to prolong microbubble transit time through the coronary circulation.[9]

The introduction of gas emboli is often unpreventable, and treatment options such as hyperbaric oxygen therapy are of limited utility. An investigation into the effects of glycocalyx injury on embolism bubble adhesion and use of pharmacologic agents targeted to reduce blood flow obstruction is warranted. A potential therapy is the intravascular administration of exogenous surface-active agents, which have been shown to decrease bubble adhesion to the vessel wall,[10] accelerate vessel reperfusion,[11,12] and attenuate thrombin formation[13] and platelet binding interactions otherwise provoked by gas microbubbles.[14]

Our study investigated the hypothesis that glycocalyx degradation alters intravascular bubble deposition patterns and subsequent dynamics to yield proximal and long-duration vessel occlusion. We also hypothesized that there are differential effects of surfactants to promote distal bubble displacement favoring more rapid reabsorption and that these depend in part on the state of the glycocalyx.

We tested these hypotheses in the rat cremaster circulation using either a saline control microinfusion or a heparinase microinfusion to degrade the glycocalyx within the cremaster microcirculation and with one of two surfactant solutions (Perftoran [OJSC SPC Perftoran, Moscow, Russia], a perfluorocarbon-based emulsion; and Pluronic F-127 [Molecular Probes, Eugene, OR], a nonionic block copolymer) or saline as a control given before embolization. Using intravital microscopy, we measured bubble dimensions after entrapment and bubble conformational and positional changes after lodging. We determined the effects glycocalyx injury and surfactant administration to alter bubble deposition and clearance.

Materials and Methods

Animal Experiments

Experiments were conducted with adult male Wistar rats (250–325 g) handled according to National Institutes of Health guidelines. The University of Pennsylvania Animal Care and Use Committee in Philadelphia, Pennsylvania, approved the study. Our intact cremaster surgical protocol and muscle preparation, except for

* Associate Professor, Department of Anesthesiology and Critical Care, Institute for Medicine and Engineering, and Institute for Translational Medicine and Therapeutics, † Research Assistant, Department of Anesthesiology and Critical Care, The University of Pennsylvania.

Received from the Department of Anesthesiology and Critical Care, The University of Pennsylvania, Philadelphia, Pennsylvania. Submitted for publication May 31, 2006. Accepted for publication July 28, 2006. Supported by grant No. R01 HL60230 from the National Heart, Lung and Blood Institute, Bethesda, Maryland.

Address correspondence to Dr. Eckmann: Department of Anesthesiology and Critical Care, University of Pennsylvania, 3400 Spruce St.-HUP, Philadelphia, Pennsylvania 19104. eckmanndm@uphs.upenn.edu.

microperfusion, as well as our use of intravital microscopy and videomicrometry, have been described in detail.[11,12,15,16] A critical aspect of our preparation is placement of a femoral artery microcatheter such that the ipsilateral cremaster microcirculation blanches upon saline injection. This preparation provides a reliable method of introducing gas embolism bubbles directly into the cremaster arteriolar microcirculation.

Surgical Preparation

Anesthesia was induced (5%) and maintained (1.2%) with inhaled halothane delivered in 30% oxygen (balance nitrogen). Anesthetized rats were placed supine on a clear acrylic tray, intubated through a tracheostomy, and ventilated. Arterial blood pressure and heart rate were monitored with a right carotid artery catheter. Intravenous fluids and drugs were administered through a left jugular venous catheter. A left femoral artery catheter was inserted for injection of air bubbles directly into the cremaster circulation. Body temperature was maintained at 35°–36°C with a heating pad and monitored with a rectal thermometer.

The cremaster muscle was exposed and dissected away from the surrounding tissue and organ using a midline scrotal incision. The muscle was spread over a transparent pedestal, and multiple sutures were attached to hold the muscle flat on the platform. The cremaster was superfused at 2 ml/min with a warmed (36°C), gassed (5% CO_2–95% N_2) Krebs buffer. The cremaster muscle was left to equilibrate for 30 min before the start of any experimentation. The cremaster temperature was monitored using an intramuscular thermocouple placed away from areas of interest. A series of clearly visible consecutive branching arteriolar vessels was selected, and other local arterial vessels were cauterized. This created a more direct vascular pathway for air embolism observation while maintaining a physiologic environment.

Microperfusion

Micropipettes were drawn from glass capillary tubes to a tip OD of 7–10 μm. Tips were ground to a 30° bevel angle on two sides. Micropipettes were cleaned after beveling by immersion in 50% nitric acid for 12 h and rinsed vigorously multiple times with deionized water. Micropipettes were backfilled with microperfusion solution before vessel puncture and then placed into a pipette holder equipped with a side port connected to the pressure outlet of a nitrogen-driven microinjector picospritzer (Model PLI-100; Medical Systems Corp., Greenvale, NY). The micropipette assembly was held in a micromanipulator mounted to the microscope stage, and the micropipette tip was viewed under the microscope. The micropipette tip was inserted into the arterial vessel feeding the cremaster circulation. The microperfusion solutions were heparinase (1 U/ml in normal saline; Sigma, St. Louis, MO) and normal saline as a control. The solution was delivered by pressure pulse ejection with a duration of 1.5 s, an ejection frequency of 0.6 s, and an off period of 0.2 s.[17] Microperfusion lasted 8–10 min, and free flow of blood was allowed for another 10 min before any embolization experiments were begun.

Preparation Stability

To demonstrate that robust vascular responses were preserved after cremaster muscle preparation and again after microperfusion, a 0.5-ml bolus of 10^{-4} M acetylcholine (Sigma Chemicals), diluted in Krebs buffer, was deposited topically to confirm the presence of endothelial mediated vasodilation. A 0.5-ml bolus of 10^{-4} M phenylephrine (Sigma Chemicals), diluted in Krebs buffer and deposited topically, was used to confirm smooth muscle–mediated constriction. More than 10 min elapsed between the applications of each vasoactive agent. Tissue responses were considered intact if the acetylcholine elicited at least a 50% increase in vessel diameter from baseline and the phenylephrine elicited at least a 20% decrease in diameter. All preparations met these criteria.

Treatment Randomization

Animals were randomly assigned to one of six groups (n = 6 per group), which were studied for the different combinations of microinfusion (heparinase or saline) and surfactant treatment. Animals first received the microperfusion solution followed by administration of the treatment compound. The three surfactant treatment regimens were comprised of two study compounds, Perftoran and Pluronic F-127, with normal saline administration as a control. Two different surfactants were used to seek any differential effects on bubble lodging and reabsorption not simply explained by a surface tension effect. Compound dosing was designed to maintain a constant surface tension effect for the two surfactants by using concentrations that reduce blood surface tension midway between its native value (approximately 52 mN/m) and that of the neat (or pure) surfactant.[11,12] Animals were given an intravenous bolus of either 0.9% NaCl, undiluted, freshly thawed (second thaw) Perftoran warmed to room temperature, or Pluronic F-127 diluted 1:9 with 0.9% NaCl. The injectate volume was calculated to be 10% of the animal's estimated blood volume (64 ml/kg for rats). For Perftoran and Pluronic F-127, this provided 1 and 0.1 vol% concentrations, respectively, in circulating blood. These concentrations were used for *in vitro* studies of thrombin production[13] and platelet binding[14] with gas embolization.

Air Embolization

Gas embolization occurred 10 min after completion of treatment (surfactant) compound delivery. Single air

bubbles were injected into the femoral artery ipsilateral to the selected cremaster as performed previously.[11,12,15] A 3-μl bubble was injected, and this volume was increased in 1-μl increments, if necessary, in subsequent injections until a suitably sized embolism arrived in the cremaster circulation. The maximum bubble volume required for successful embolization was 5 μl. Once a bubble successfully embolized the cremaster, no other experiments were conducted using that animal.

Data Analysis

Data analysis was performed using the videotaped recording of each experiment with a calibrated video micrometer as previously described.[11,12,15,16] If two or more bubbles lodging adjoined at one location, they were considered to be a single embolism, and in that case, the total embolism volume was calculated as the sum of the individual bubble volumes.

Bubble length, L, and average diameter, D, were measured after initial entrapment. Bubble volume and aspect ratio (length/radius) were then calculated, assuming the elongated bubble is approximated by a cylinder with hemispherical end caps.[11,12,15,16,18,19] The total bubble surface area was calculated as the sum of the areas of the end caps (πD^2) plus the cylindrical central portion (πDL) of each bubble. The absorption times predicted for bubbles ($T_{predicted}$) were computed based on the measured initial bubble dimensions using the mathematical model described by Branger and Eckmann[15] and used subsequently.[11,12,16,18] $T_{observed}$, the elapsed time actually required for the last remaining observable remnant of a bubble to reabsorb from the embolized vessel, was determined from the videomicroscopy recording. We calculated the percent change in observed (actual) absorption time from the time predicted, $\Delta T\%$, to be:

$$\Delta T\% = \frac{T_{predicted} - T_{observed}}{T_{predicted}} \times 100\% \qquad (1)$$

Bubble entrapment was followed by "stick-and-slip" episodes marking the motion of large sliding interfaces and resulting from strong collective interfacial interactions of large numbers of surface molecules. Stick-and-slip events occur as surface interactions weaken, signaling a transition from arrested to free motion of the surfaces relative to one another.[20] Stick-and-slip events were quantitatively assessed by counting the number of episodes of bubble lodging and subsequent bubble sliding in the first 2 min after initial entrapment and by measuring the distance traveled during each slip event.[12] Only bubble motion lasting longer than 1 s during which the bubble traveled more than one vessel diameter downstream counted as a stick-and-slip event. The distance traveled was normalized to the local vessel diameter.

Statistical Analysis

Results are presented as the arithmetical mean ± SD. Normality of all data was confirmed using the D'Agostino-Pearson omnibus test. Group variances were examined using the F test. With equal variances, statistical significance between groups was established using analysis of variance, with $P < 0.05$ considered statistically significant using the Bonferroni correction. Because the variances were not equal for analysis of the distance bubbles traveled in stick and slip behavior, the *t* test for unequal variances was used to compare specific group means.

Results

Hemodynamic Stability and Baseline Vessel Tone

Heart rate and blood pressure data before, midway through, and 5 min after infusion of the microperfusion solution and the surfactant compounds were not different between groups. Use of either heparinase or saline had no significant effect on arteriolar tone or reactivity. There was no appreciable change in second- or third-order arteriole diameter after microperfusion or surfactant delivery.

Initial Bubble Lodging and Bubble Dynamics

Air emboli (range, 3.9–9.9 nl) lodged in the cremaster microvasculature quickly after injection. Either a single bubble or two adjacent bubbles (one case) formed the embolism. There was a linear correlation between embolism volume and vessel diameter, as shown in figure 1. The microperfusion data segregated into two distinct relations. Mean values and bidirectional error bars for the data are plotted along with linear regression lines based on the mean values. The regression lines were forced through the origin based on the physical requirement that bubbles with extremely small volumes can only obstruct vessels of very small diameter. With heparinase microperfusion, bubbles had larger volumes ($P < 0.003$) and lodged in larger vessels ($P < 0.001$) than with saline microperfusion. The correlation coefficients were large ($R \geq 0.974$), and the regression line slopes were different (12.90 *vs.* 9.75; $P < 0.05$), indicating a strong dependence of bubble lodging on the state of the glycocalyx.

Mean values for bubble volumes, embolized vessel diameters, initial bubble length, and initial aspect ratio are presented in table 1 for each group. Values were not different based on microperfusion. Bubble length and aspect ratio depended on the surfactant treatment. Volumes were smallest in the Pluronic F-127 groups compared with either saline controls or Perftoran ($P < 0.0083$). Bubble volume was smaller with Perftoran compared with saline ($P < 0.0083$). The mean diameter of emboli was smallest for Pluronic F-127 ($P < 0.0083$

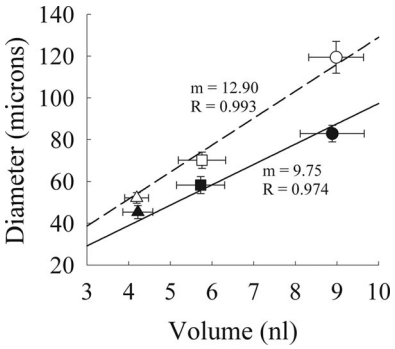

Fig. 1. Entrapping vessel diameter in relation to the gas embolism bubble volume. Ensemble means with bidirectional SD error bars are shown for groups of animals receiving microinfusion–surfactant combinations of saline–saline (●), saline–Perftoran (■), saline–Pluronic F-127 (▲), heparinase–saline (○), heparinase–Perftoran (□), and heparinase–Pluronic F-127 (△). Linear regression lines are forced through the origin (see text) and have different slopes for saline microinfusion (——) and heparinase microinfusion (- - - -).

compared with saline and Perftoran). Bubble volume was smaller after Perftoran compared with saline ($P < 0.0083$). The initial bubble aspect ratio was largest for Pluronic F-127 ($P < 0.0083$ compared with saline and Perftoran), and the aspect ratio was larger for Perftoran than for saline ($P < 0.0083$).

Bubble surface area after lodging is shown in figure 2. Total surface area was smaller with saline microperfusion and Pluronic F-127 than with double saline control dosing ($P < 0.0056$). With heparinase microperfusion, total surface area was independent of surfactant treatment. With Perftoran or saline control as the surfactant, surface area was smallest for heparinase compared with saline microperfusion ($P < 0.0056$). End cap surface area was larger, and surface area of the cylindrical bubble portion was smaller, for heparinase microperfusion and saline dosing compared with the double saline control condition ($P < 0.0056$).

Vessel diameter decreased slightly in the first 5–10 s after bubble lodging, with vessels constricting less than 5%. Group means ranged from 2.5 ± 1.3% (heparinase–saline) to 3.7 ± 1.1% (saline–Pluronic F-127). Bubble length increased slightly, ranging from 4.7 ± 2.1% (heparinase–saline) to 7.5 ± 2.6% (saline–Pluronic F-127). The aspect ratio increased 7–8% per group. These changes in bubble dimensions were not significant ($P > 0.62$ in all cases).

The occurrence of stick-and-slip events was greatest in both the Pluronic F-127 and Perftoran treatment groups after either saline or heparinase microinfusion. Bubbles in these groups displaced further distally than did bubbles in the saline control group after either microinfusion ($P < 0.0056$). Table 2 shows the average number of stick-and-slip events as defined. In the saline–saline and heparinase–saline groups, bubbles traveled approximately 0.5–1.5 bubble lengths (with a bubble aspect ratio of approximately 12–40) per event, as shown in figure 3. Bubbles in both the Pluronic F-127 and Perftoran groups traveled a far greater normalized slip distance, regardless of the microinfusion type ($P < 0.009$). Coupling the absolute number of slip events with the distance traveled per event shows that bubbles in the surfactant groups dislodged and moved distally 7–22 times further than saline controls. This corresponds to a displacement of approximately 1–3 cm compared with only 1–1.5 mm for the saline–saline and heparinase–saline controls.

Bubble Reabsorption and Reperfusion

Reabsorption times predicted by equation 1 and observed in the experiment are presented along with linear regression analysis in figure 4. The regression lines were forced through the origin based on the expectation that extremely small bubbles reabsorb in a very short time.[15,19] The two data clusters for the saline–saline and heparinase–saline conditions overlapped, yielding two indistinct regression lines (hence only one can be seen in fig. 4) with essentially the same slope (1.002 for saline–saline and 1.005 for heparinase–saline) as the line of identity. This indicates that the state of the glycocalyx did not affect the physics of bubble reabsorption beyond its influence on the location of bubble lodging. The large correlation coefficients ($R > 0.94$ for both of these cases) show that the reabsorption times measured collectively were individually closely predicted. The separate measure of the percent deviation between the two values calculated with equation 1 as presented in table 2 further supports this. The slopes of the remaining four regression lines shown in figure 4 ranged from 1.37 to

Table 1. Bubble Geometry at Initial Entrapment

Treatment Group, Micropuncture–Surfactant	Bubble Volume, nl	Bubble Diameter, μm	Bubble Length, μm	Bubble Aspect Ratio
Saline–saline	8.9 ± 0.8	82.2 ± 4.6	1,622 ± 103	39.7 ± 4.3
Saline–Perftoran	5.7 ± 0.6*	58.3 ± 4.1*	2,119 ± 251	73.4 ± 13.0*
Saline–Pluronic F-127	4.2 ± 0.4*†	45.3 ± 3.1*†	2,925 ± 168*	115.1 ± 14.5*†
Heparinase–saline	9.0 ± 0.7	119.4 ± 7.6*	726 ± 73*	12.3 ± 1.9*
Heparinase–Perftoran	5.8 ± 0.6‡	70.2 ± 3.9‡	1,440 ± 141‡	41.2 ± 3.1‡
Heparinase–Pluronic F-127	4.2 ± 0.3‡§	52.1 ± 2.6‡§	1,941 ± 206‡	74.9 ± 10.7‡§

* $P < 0.0083$ compared with saline–saline. † $P < 0.0083$ compared with saline–Perftoran. ‡ $P < 0.0083$ compared with heparinase–saline. § $P < 0.0083$ compared with heparinase–Perftoran.

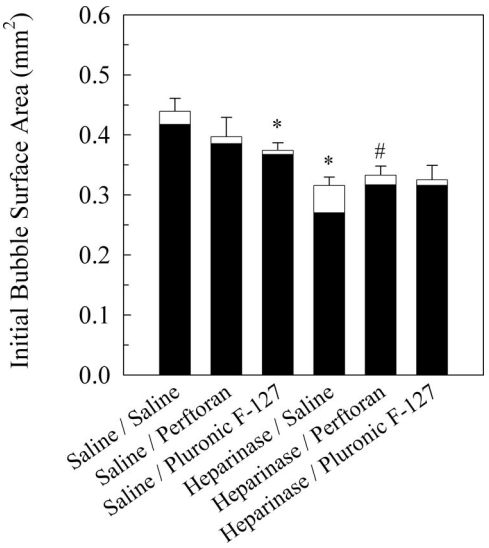

Fig. 2. Initial total bubble surface area after gas embolization for different microinfusion–surfactant combinations. Total surface area is comprised of bubble end cap surface area (*unshaded region*) and bubble cylindrical core surface area (*shaded region*). Statistical analysis showed total area to be different for saline–Pluronic F-127 and heparinase–saline treatment compared with saline–saline treatment (* $P < 0.0056$) and for heparinase–Perftoran treatment compared with saline–Perftoran treatment (# $P < 0.0056$).

2.27, with all $R > 0.91$. These slopes were all different from the line of identity ($P < 0.01$), indicating that with a surfactant, the observed reabsorption times were always faster than predicted. This correlates well with the percent deviation calculated with equation 1 and reported in table 2. For Pluronic F-127 and Perftoran, reabsorption was significantly faster than predicted for both saline and heparinase microinfusion, with Pluronic F-127 also promoting reabsorption faster than Perftoran. This is evident in table 2 and figure 4, in which the Pluronic F-127 data are leftward (steeper slope) of the Perftoran and saline control data.

We replotted data from Figure 4 in figure 5 to illustrate the relation between the observed clearance time and initial bubble surface area.[12,15] The accompanying linear regression analysis was forced through the origin because minute bubbles (extremely small surface area) are expected to reabsorb fast. For both microinfusions, the two regression line slopes for the corresponding Pluronic F-127 and Perftoran treatment were different ($P < 0.0083$). The slopes for the saline control groups were nearly double (Perftoran) and triple (Pluronic F-127) the surfactant groups for the corresponding saline and heparinase microinfusion conditions. This indicates that for fixed bubble surface area, clearance took nearly three times longer (Pluronic F-127) or twice as long (Perftoran) if a surfactant were not given before gas embolization.

Discussion

Clinically applicable methods of prevention and treatment for gas embolism based on an understanding of the interfacial interactions involved could result in a pharmacologic treatment to reduce morbidity, mortality, and associated care costs. Gas embolization can obstruct blood flow, elicit ischemia, promote thromboinflammatory responses, and injure or denude the endothelium, all of which are harmful to brain and heart or other end organs.[21,22] Embolism bubble entrapment results from an adhesion interaction between the bubble and the luminal, exposed endothelial cell surface. The native endothelial cell surface layer, or glycocalyx, is a heterogeneous amalgam of macromolecules that plays an important role as a mechanotransducer of local stresses[23,24] as a regulator of platelet[25] and leukocyte[26,27] binding, in the regulation of microvascular hematocrit,[17] and it influences erythrocyte deformation and motion through capillaries.[28] The glycocalyx has been shown to have a role in establishing cerebral microvascular blood flow resistance.[29] The structure and composition of the endothelial surface layer confer its "antiadhesive" nature that provides barrier function for solute and water transport across the vessel lumen and lends to its role in the regulation of fibrinolysis and coagulation.[30,31]

Relevant to gas embolism events and our investigation, preexisting disruption of the endothelial glycocalyx surface layer may enhance the "adhesiveness" of the endothelial surface for bubbles, as suggested previously.[9] Heparinase administration by large intravenous bolus[29] or by vessel micropuncture and microinfusion such as we and others[17,27] have performed is an established method of degrading the glycocalyx. Heparinase reduces the glycocalyx thickness by 43%,[29] but the adhesive nature of heparinase-, hypoxia-, ischemia–reperfusion-, or cardioplegia-damaged endothelial surface layer has

Table 2. Bubble Motion and Clearance Relative to Predicted Lifetime

Treatment Group, Micropuncture–Surfactant	Number of Stick and Slip Episodes	Mean ΔT%	SD ΔT%
Saline–saline	0.5 ± 0.6	0.7	2.7
Saline–Perftoran	5.7 ± 1.2*	36.2*	3.1
Saline–Pluronic F-127	6.8 ± 1.5*	56.1*	3.4
Heparinase–saline	0.7 ± 0.5	0.2	5.5
Heparinase–Perftoran	4.3 ± 1.0†	27.3†	4.8
Heparinase–Pluronic F-127	4.8 ± 0.8†	40.1†	5.2

* $P < 0.01$ compared with saline–saline. † $P < 0.01$ compared with heparinase–saline.

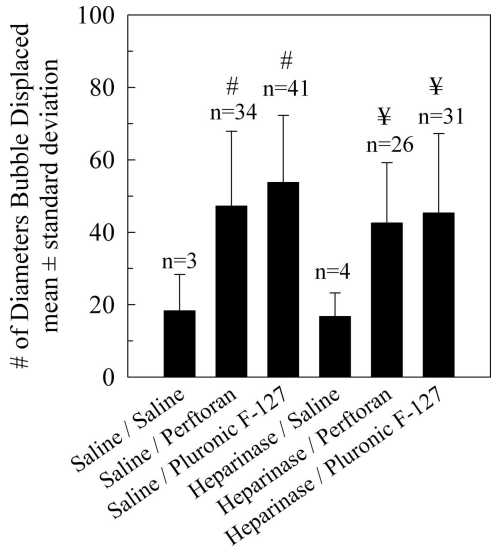

Fig. 3. Normalized bubble displacement distances traveled during slip events for different microinfusion–surfactant combinations. Statistical analysis showed displacement distances to be larger for saline–Perftoran and saline–Pluronic F-127 than for saline–saline (# $P < 0.0056$) and larger for heparinase–Perftoran and heparinase–Pluronic F-127 than for heparinase–saline (¥ $P < 0.0056$).

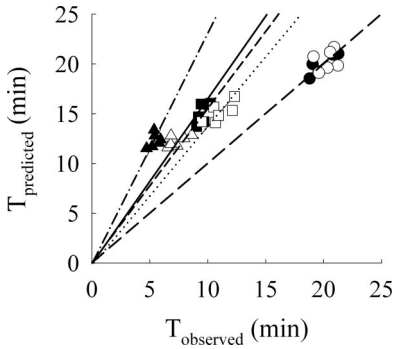

Fig. 4. Relation between the measured elapsed time ($T_{observed}$) and the predicted time ($T_{predicted}$) required for the last remaining observable remnant of parent bubbles to clear from the embolized vessel. Linear regression lines are forced through the origin (see text). Symbols are for microinfusion–surfactant combinations of saline–saline (●), saline–Perftoran (■), saline–Pluronic F-127 (▲), heparinase–saline (○), heparinase–Perftoran (□), and heparinase–Pluronic F-127 (△). Regression line types for microinfusion–surfactant combinations are saline–saline (*longer dashed line*), saline–Perftoran (*shorter dashed line*), saline–Pluronic F-127 (*dashed and dotted line*), heparinase–saline (overlaps *longer dashed line*), heparinase–Perftoran (*dotted line*), and heparinase–Pluronic F-127 (*solid line*).

not been previously determined. In these *in vivo* experiments, we have used intravital microscopy to quantify the effects of heparinase microinfusion and surfactant delivery, alone or in combination, on air embolism bubble deposition into, and clearance from, the arterial microcirculation.

The use of heparinase was expected to increase adhesiveness of the endothelial surface and result in more proximal lodging of embolism bubbles. We found that bubbles did lodge in larger diameter (*i.e.*, more proximal) regions of the microcirculation after heparinase microinfusion compared with saline microinfusion (fig. 1 and table 1). Depending on the surfactant administration conditions, the average embolized vessel diameter was anywhere from 15% (Pluronic F-127) to 45% (saline) larger if the glycocalyx was degraded.

Surfactants were expected to lead to deposition of smaller bubbles into more distal vessels and to accelerate clearance. Both surfactants decreased bubble volume (fig. 1 and table 1), with Pluronic F-127 exerting a greater effect than Perftoran for the same surface tension target. The greater effect of Pluronic F-127 was evident in the smaller diameter of the vessel that was embolized (fig. 1 and table 2), smaller surface area (fig. 2), shorter duration for which bubbles remained lodged in one location (fig. 3 and table 2), greater distance bubbles moved with each slip episode (fig. 3 and table 2), and faster time to complete vessel reperfusion (figs. 4 and 5 and table 2).

For gas embolization preceded by surfactant administration, the gas volume lodging was approximately 45% (Pluronic F-127) or approximately 30–35% (Perftoran) smaller than if saline were given. This is likely a primary effect of small bubbles snapping off from the injected bubble to enter the cremaster circulation and has been both predicted[32] and observed *in vivo*.[11] The smaller bubbles in the surfactant groups lodged more distally. With the exception of the combination of saline microinfusion and Pluronic F-127, the total surface area profile remained constant within each microinfusion group. The differences observed in end cap surface area are an indicator of the vessel diameter, because end cap surface area depends only on D. Except for the heparinase–saline condition, the end cap surface area contributes only 1.7–4.8% of the total surface area, leaving the central cylindrical portion of the bubble to contribute approximately 95–98% of the total surface area (fig. 2). The 14% contribution of the end cap area to the total in the heparinase–saline group is reflective of the very proximal bubble entrapment. With otherwise similar surface areas but smaller volumes, our finding that bubbles in the surfactant groups reabsorb faster by diffusion of a smaller volume of gas across an equal surface area is expected (fig. 5). This result does not account for the enhanced distal bubble travel associated with surfactant administration.

The finding that the number and magnitude of stick-and-slip events are different in the study groups suggests that the adhesion forces developed between the bubble surface and the vessel wall are dependent on both the state of the glycocalyx and the particular surfactant used. The loss of the "antiadhesive" quality of the glycocalyx is marked by more proximal bubble entrapment in all the heparinase microinfusion groups compared with their saline microinfusion controls (fig. 1 and table 1) as well as by the positive effect of the surfactants to enhance the

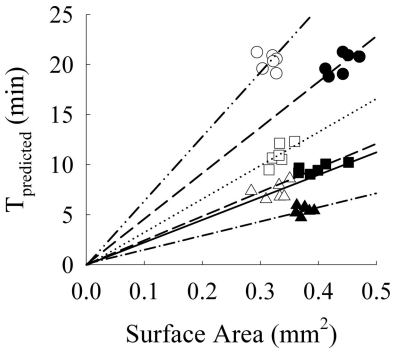

Fig. 5. Relation between initial bubble surface area and the actual elapsed time ($T_{observed}$) required for the last remaining observable remnant of parent bubbles to clear from the embolized vessel. Linear regression lines are forced through the origin (see text). Symbols are for microinfusion–surfactant combinations of saline–saline (●), saline–Perftoran (■), saline–Pluronic F-127 (▲), heparinase–saline (○), heparinase–Perftoran (□), and heparinase–Pluronic F-127 (Δ). Regression line types for microinfusion–surfactant combinations are saline–saline (*longer dashed line*), saline–Perftoran (*shorter dashed line*), saline–Pluronic F-127 (*dashed and dotted line*), heparinase–saline (*dashed and double dotted line*), heparinase–Perftoran (*dotted line*), and heparinase–Pluronic F-127 (*solid line*). Regression line slopes for saline (surfactant controls) groups are nearly double (Perftoran) or triple (Pluronic F-127) the surfactant groups for the corresponding microinfusion conditions. This indicates that bubble clearance takes two to three times longer if a surfactant is not given before gas embolization.

frequency of stick-and-slip episodes and the magnitude of bubble travel during slip events (fig. 2). We have restricted the analysis of bubble detachment and distal travel to the first 2 min after embolization because this permitted comparison of events across the six groups studied.

The force of adhesion established by the bubble surface contacting the vessel wall retards bubble motion.[1] The only driving force promoting bubble displacement without blood flow is the pressure difference across the bubble acting on the cross sectional area profile of the bubble in the direction of the vessel axis. Because neither systemic blood pressure nor vessel diameter changed after bubble entrapment, the driving pressure and cross-sectional area remained constant. Therefore, a decrease in the local adhesion force, a decrease in the bubble surface area contacting the vessel wall, or some combination thereof must lead to a net reduction in the adhesion force. We have previously shown that various surfactants alter these adhesion forces[10] and can lead to more rapid clearance of embolism bubbles in cases in which the glycocalyx has been left intact.[11,12] The ability of the surfactants to attenuate the adhesion forces and permit distal entrapment and bubble slip has several underpinnings, including direct competition with proteins for interfacial occupancy, interference with formation of adhesion interactions between the cell and bubble surfaces involved, and possibly direct interaction with the native or remnant (after heparinase) structural elements of the glycocalyx. The two compounds we have used in this study are a nonionic polyol (Pluronic F-127) and a perfluorocarbon (Perftoran), which are chemically dissimilar. Perftoran is an emulsion of perfluorodecalin ($C_{10}F_{18}$) and perfluoromethylcyclohexylpiperiden ($C_{12}F_{23}N$). Currently, it is neither approved by the US Food and Drug Administration nor being tested in any clinical trials in the United States. Pluronic F-127 is a block copolymer that has one hydrophobic polypropylene chain and two hydrophilic polyethylene oxide chains. This compound is approved by the Food and Drug Administration as an additive to drug formulations to improve intracellular delivery. In previous studies, we have demonstrated that Perftoran enhances embolism bubble clearance with an intact glycocalyx[12] and that both Perftoran and Pluronic-127 attenuate thrombin formation[13] and platelet binding[14] using *in vitro* models of gas embolization.

Bubbles in the surfactant groups cleared the microcirculation sooner with faster return of blood flow than occurred in the saline control groups (figs. 4 and 5). This was the result of gas reabsorption and bubble movement out to the periphery and has been described in detail.[12] Briefly bubbles become elongated and slender, increasing surface area for gas transport out of the bubble, as they move distally. Bubbles in the surfactant groups continued to stick and slip after the initial 2-min evaluation period until small bubbles passed transcapillary into the venous circulation. The associated arteriolar blood flow returned faster than predicted in these groups (figs. 4 and 5 and table 2).

Our results indicated that the glycocalyx plays an important role in mediating the location of embolism bubble entrapment and the accompanying duration of blood flow obstruction. The addition of surfactants before embolization did significantly attenuate the duration of blood flow obstruction.[12] For dosing based on a comparable surface tension effect, Pluronic F-127 had a greater effect than Perftoran to decrease bubble size, promote more distal embolization, and speed reestablishment of blood flow throughout the experiments with and without glycocalyx destruction. This pharmacologic targeting in anticipation of bubble adhesion to the endothelial surface may provide a potential novel preemptive approach to gas embolism treatment.

References

1. Suzuki A, Eckmann DM: Embolism bubble adhesion force in excised perfused microvessels. ANESTHESIOLOGY 2003; 99:400–8
2. Muth CM, Shank ES: Gas embolism. N Engl J Med 2000; 342:476–82
3. Forlee MV, Grouden M, Moore DJ, Shanik G: Stroke after varicose vein foam injection sclerotherapy. J Vasc Surg 2006; 43:162–4
4. Hieber C, Ihra G, Nachbar S, Aloy A, Kashanipour A, Coraim F: Near-fatal paradoxical gas embolism during gynecological laparoscopy. Acta Obstet Gynecol Scan 2000; 79:898–9
5. Mitchell SJ, Benson M, Vadlamudi L, Miller P: Cerebral arterial gas embolism by helium: An unusual case successfully treated with hyperbaric oxygen and lidocaine. Ann Emerg Med 2000; 35:300–3

6. Ward BJ, Donnell JL: Hypoxia induced disruption of the cardiac endothelial glycocalyx: Implications for capillary permeability. Cardiovasc Res 1993; 27: 384–9

7. Keller MW, Geddes L, Spotnitz W, Kaul S, Duling BR: Microcirculatory dysfunction following perfusion with hyperkalemic, hypothermic, cardioplegic solutions and blood reperfusion: Effects of adenosine. Circulation 1991; 84: 2485–94

8. Beresewicz A, Czarnowska E, Maczewski M: Ischemic preconditioning and superoxide dismutase protect against endothelial dysfunction and endothelium glycocalyx disruption in the postischemic guinea-pig hearts. Mol Cell Biochem 1998; 186:87–97

9. Lindner JR, Ismail S, Spotnitz WD, Skyba DM, Jayaweera AR, Kaul S: Albumin microbubble persistence during myocardial contrast echocardiography is associated with microvascular endothelial glycocalyx damage. Circulation 1998; 98:2187–95

10. Suzuki A, Armstead SC, Eckmann DM: Surfactant reduction in embolism bubble adhesion and endothelial damage. ANESTHESIOLOGY 2004; 101:97–103

11. Branger AB, Eckmann DM: Accelerated arteriolar gas embolism reabsorption by an exogenous surfactant. ANESTHESIOLOGY 2002; 96:971–9

12. Eckmann DM, Lomivorotov VN: Microvascular gas embolization clearance following perfluorocarbon administration. J Appl Physiol 2003; 94:860–8

13. Eckmann DM, Diamond SL: Surfactants attenuate gas embolism-induced thrombin production. ANESTHESIOLOGY 2004; 100:77–84

14. Eckmann DM, Armstead SC, Mardini F: Surfactant reduces platelet-bubble and platelet-platelet binding induced by *in vitro* air embolism. ANESTHESIOLOGY 2005; 103:1204–10

15. Branger AB, Eckmann DM: Theoretical and experimental intravascular gas embolism absorption dynamics. J Appl Physiol 1999; 87:1287–95

16. Eckmann DM, Kobayashi S, Li M: Microvascular embolization following polidocanol microfoam sclerosant administration. Dermatol Surg 2005; 31:636–43

17. Desjardins C, Duling BR: Heparinase treatment suggests a role for the endothelial cell glycocalyx in regulation of capillary hematocrit. Am J Physiol 1990; 258:H647–54

18. Sta. Maria N, Eckmann DM: Model predictions of gas embolism growth and reabsorption during xenon anesthesia. ANESTHESIOLOGY 2003; 99:638–45

19. Branger AB, Lambertsen CJ, Eckmann DM: Cerebral gas embolism absorption during hyperbaric therapy: Theory. J Appl Physiol 2001; 90:593–600

20. Rozman MG, Urbakh M, Klafter J: Stick-slip dynamics as a probe of frictional forces. Europhys Lett 1997; 39:183–8

21. Engelman R: The neurologic complications of cardiac surgery: Introduction. Semin Thorac Cardiovasc Surg 2001; 13:147–8

22. Mitchell S, Gorman D: The pathophysiology of cerebral arterial gas embolism. J Extra Corpor Technol 2002; 34:18–23

23. Florian JA, Kosky JR, Ainslie K, Pang Z, Dull RO, Tarbell JM: Heparan sulfate proteoglycan is a mechanosensor on endothelial cells. Circ Res 2003; 93:e136–42

24. Tarbell JM, Pahakis MY: Mechanotransduction and the glycocalyx. J Int Med 2006; 259:339–50

25. Vink H, Constantinescu AA, Spaan JAE: Oxidized lipoproteins degrade the endothelial surface layer: Implications for platelet-endothelial cell adhesion. Circulation 2000; 101:1500–2

26. Soler M, Desplat-Jego S, Vacher B, Ponsonnet L, Fraterno M, Bongrand P, Martin J, Foa C: Adhesion-related glycocalyx study: Quantitative approach with imaging-spectrum in the energy filtering transmission electron microscope. FEBS Lett 1998; 429:89–94

27. Mulivor AW, Lipowsky HH: Role of glycocalyx in leukocyte-endothelial cell adhesion. Am J Physiol 2002; 283:H1282–91

28. Damiano ER: The effect of the endothelial-cell glycocalyx on the motion of red blood cells through capillaries. Microvasc Res 1997; 55:77–91

29. Vogel J, Sperandio M, Pries AR, Linderkamp O, Gaehtgens P, Kuschinsky W: Influence of the endothelial glycocalyx on cerebral blood flow in mice. J Cereb Blood Flow Metab 2000; 20:1571–8

30. Pries AR, Secomb TW, Gaehtgens P: Biophysical aspects of blood flow in the microvasculature. Cardiovasc Res 1996; 32:654–67

31. Pries AR, Secomb TW, Gaehtgens P: The endothelial surface layer. Pflugers Arch 2000; 440:653–66

32. Tsai TM, Miksis MJ: The effects of surfactant on the dynamics of bubble snap-off. J Fluid Mech 1997; 337:381–410